



Universiteit
Leiden
The Netherlands

Design and synthesis of paramagnetic probes for structural biology

Liu, W.

Citation

Liu, W. (2013, November 25). *Design and synthesis of paramagnetic probes for structural biology*. Retrieved from <https://hdl.handle.net/1887/22357>

Version: Not Applicable (or Unknown)

License: [Leiden University Non-exclusive license](#)

Downloaded from: <https://hdl.handle.net/1887/22357>

Note: To cite this publication please use the final published version (if applicable).

Cover Page



Universiteit Leiden



The handle <http://hdl.handle.net/1887/22357> holds various files of this Leiden University dissertation.

Author: Liu, Wei-Min

Title: Design and synthesis of paramagnetic probes for structural biology

Issue Date: 2013-11-25

Chapter II

A pH sensitive, colorful, lanthanoid-chelating paramagnetic NMR probe

Based on the research article:

Liu, W. -M.; Keizers, P. H. J.; Hass, M. A. S.; Blok, A.; Timmer, M.; Sarris, A. J. C.; Overhand, M.; Ubbink, M. "A pH-sensitive, Colorful, Lanthanide-chelating Paramagnetic NMR Probe" *J. Am. Chem. Soc.* **2012**, *134*, 17306-17313.

Abstract

Paramagnetic lanthanoid ions are broadly used in NMR spectroscopy. The effects of unpaired electrons on NMR spectral parameters provide a powerful tool for the characterization of macromolecular structures and dynamics. Here, a new lanthanoid chelating NMR probe, Caged Lanthanoid NMR Probe-7 (CLaNP-7), is presented. It can be attached to protein surfaces *via* two disulfide bridges, yielding a probe that is rigid relative to the protein backbone. CLaNP-7 extends the application range of available probes. It has a yellow color, which is helpful for sample preparation. Its effects are comparable to those of CLaNP-5, but its charge is two units lower (+1) than that of CLaNP-5 (+3), reducing the change in surface potential after probe attachment. It also has a different magnetic susceptibility tensor, so by using both tags, two sets of structural restraints can be obtained per engineered cysteine pair. Moreover, it was found that the orientation of the magnetic susceptibility tensor is pH dependent ($pK_a \sim 7$) when a histidine residue is located in the neighborhood of the probe attachment site. The results show that the His imidazole group interacts with the CLaNP-7 tag. It is proposed that the histidine residue forms a hydrogen bond to a water/hydroxyl molecule that occupies the ninth coordination position on the lanthanoid, thus breaking the two-fold symmetry of the CLaNP tag in a pH-dependent way.

Introduction

In recent years, paramagnetic probes have been used broadly in nuclear magnetic resonance (NMR) spectroscopy. The effects of unpaired electrons on NMR spectral parameters, such as pseudocontact shifts (PCSs), residual dipolar couplings (RDCs) and nuclear relaxation enhancements (PREs), have been recognized as powerful tools for the characterization of macromolecular structures and their dynamics and interactions.^{5,9,95,129-133} Among the paramagnetic effects, PCSs yield valuable long-range distance and orientation information and RDCs are distance-independent, providing information on the whole protein, making them powerful restraints to refine protein structures and determine protein orientations in complexes.¹³⁴

To yield unambiguous restraints, the paramagnetic center must be site-specifically and rigidly attached to the protein. For Ca^{2+} or Mg^{2+} containing metalloproteins, lanthanoid ions can substitute the natural metal,^{66,135,136} but most proteins are devoid of these metal binding sites. Therefore, several methods have been developed to introduce artificial paramagnetic metals into protein. For instance, metal binding peptide tags were designed that can be engineered genetically at the N or C terminus or into a loop region of a protein.^{71,74,75,101,137} Other strategies use synthetic organic thio-functional tags, which can be introduced *via* cysteine mutations.^{5,44,56}

1,4,7,10-tetraazacyclododecane-1,4,7,10-tetraacetic acid (DOTA) is a typical ligand for lanthanoid ions. The coordination of DOTA to lanthanoid ions results in two stable diastereomers, a square antiprism (SA) and a twisted square antiprism (TSA).¹³⁸⁻¹⁴¹ Each diastereomer relates to one of two possible configurations of the macrocycle rings ($\lambda\lambda\lambda\lambda$ and $\delta\delta\delta\delta$) and one of two orientations of the chelate arms (Δ and Λ). The enantiomers $\Delta\lambda\lambda\lambda\lambda$ and $\Lambda\delta\delta\delta\delta$ belong to the SA structures, whereas the pair of $\Lambda\lambda\lambda\lambda\lambda$ and $\Delta\delta\delta\delta\delta$ forms the TSA conformation. In previous studies, we have developed paramagnetic lanthanoid probes based on cyclen.^{11,36,40} The probes are attached to target proteins *via* two disulfide bridges, which strongly reduces the mobility.⁴⁰ In the most recent version, two chelating pyridine-*N*-oxide arms force the probe to exist into one diastereomer, the SA form, in the solution state.^{11,39} This results in singular NMR resonances and one magnetic susceptibility tensor. This probe, named Caged Lanthanoid NMR Probe-5 (CLaNP-5, Figure 1), showed the largest PCSs and RDCs described so far.¹¹ A drawback is the total charge of the

probe, which is 3+ after chelation with a lanthanoid ion. When CLaNP-5 is linked to a protein surface, the extra charge changes the electrostatic potential, which may affect molecular interactions with ligands and proteins. In this chapter, a new tag is described (CLaNP-7, Figure 1) that has a reduced net charge while maintaining conformational rigidity. Ln-CLaNP-7 complexes have different magnetic susceptibilities than those of CLaNP-5 and its endogenous color allows for easy detection of tagged protein. Furthermore, we show that CLaNP-7 can interact with a nearby histidine residue, causing a pH dependence of the magnetic susceptibility tensor (χ -tensor). It was shown that two sets of distance restraints can be obtained, simply by changing the pH. A model for the pH dependent interaction is proposed.

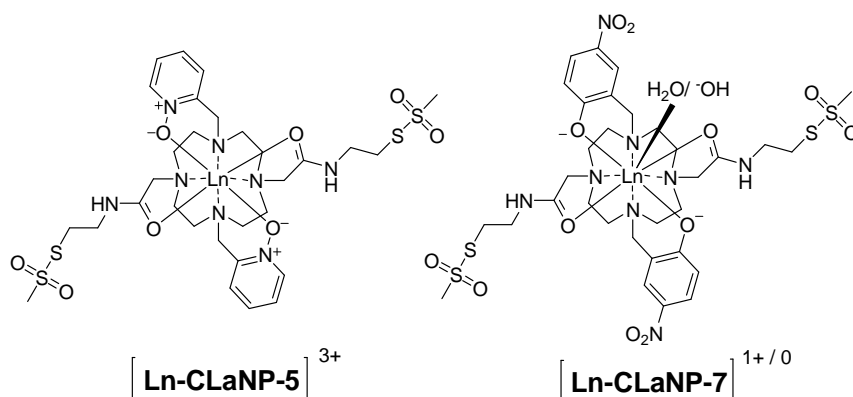


Figure 1. Structures of Ln-CLaNP-5¹¹ and Ln-CLaNP-7.

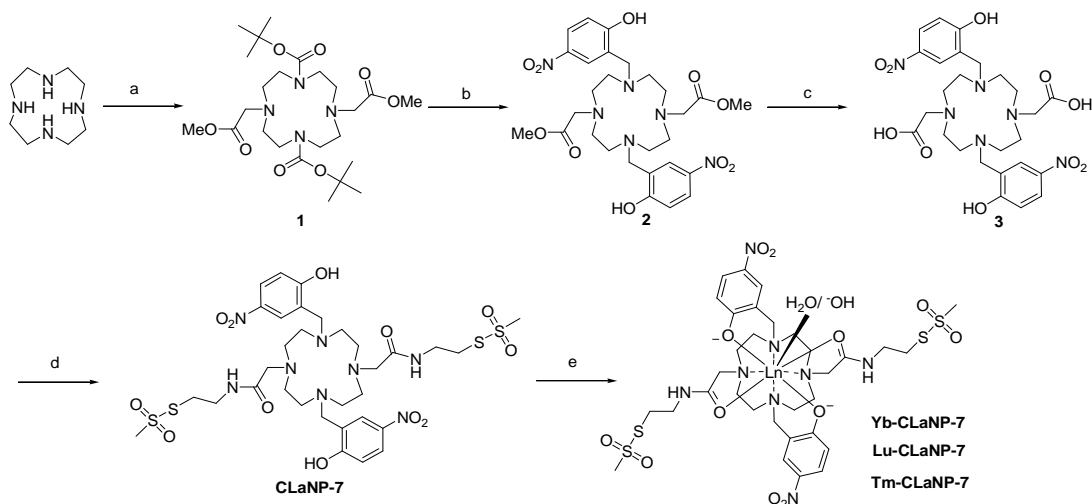
Results

Synthesis of Caged Lanthanoid NMR Probe-7 (CLaNP-7)

In 2004, Prof. A. D. Sherry's group published a study on a MRI contrast agent based on the cyclen scaffold and carrying a *p*-nitrophenol ligating group.⁴³ The crystal structure of the MRI contrast agent indicated that the phenol is deprotonated and a water molecule sits above the plane of the oxygen atoms. In order to design a rigid cyclen based probe with a reduction of net positive charge, the pyridine-*N*-oxide arms used for CLaNP-5 were replaced with *p*-nitrophenol arms (Figure 1). The *p*-nitro groups enhance the acidity of the phenolic protons and upon binding the lanthanoid, the phenol groups will be deprotonated. As the lanthanoid has a charge of +3, the net charge of the entire complex will be +1, unless a hydroxyl ion rather than a water molecule can coordinate, in which case the overall charge is zero (see

below). The two *p*-nitrophenol groups provide *C*₂-symmetry and it was anticipated that the two six-membered ring chelating systems (Figure 1) provide sufficient rigidity and thus lead to one preferred tetraazacyclododecane ring conformation.³⁹ The yellow color associated with *p*-nitrophenolate groups is convenient for the purification of tagged proteins.

The synthesis of CLaNP-7 is shown in Scheme 1. Commercially available cyclen was converted into **1** in 83% yield over two steps, in which two opposing amines were temporarily protected with *tert*-butoxycarbonyl (Boc) groups and the other two amines subsequently functionalized by reaction with methyl bromoacetate.⁴¹ Compound **1** was deprotected by trifluoroacetic acid (TFA) and reacted with 2-hydroxy-5-nitrobenzyl bromide at 80 °C to obtain **2**.^{43,142} Removal of the methyl ester group in the presence of base in 1,4-dioxane as solvent yielded **3**.¹⁴³ Condensation of **3** with excess 2-(aminoethyl)-methanethiosulfonate in presence of 1-ethyl-3-(3-dimethylaminopropyl)carbodiimide (EDC) and *N*-hydroxysuccinimide (NHS) yielded CLaNP-7 in 40% yield. The Yb-CLaNP-7, Tm-CLaNP-7 and Lu-CLaNP-7 complexes were obtained by chelating with the corresponding lanthanoid acetate salts in *N,N*-dimethylformamide (DMF). After chelation, the wavelength of the maximum absorbance shifted from 310 nm to 390 nm and the tag obtained a more intense yellow color (Figure 2A).



Scheme 1. Synthesis of CLaNP-7. (a) i) BocOSu, CHCl₃, RT 36 h; ii) methyl bromoacetate, K₂CO₃, RT, 12 h; (b) i) TFA, DCM, RT, 4 h; ii) 2-hydroxy-5-nitrobenzyl bromide, K₂CO₃, ACN, 80 °C, 12 h; (c) NaOH, 1,4-dioxane, RT, 4 h (d) aminoethyl-MTS, NHS, EDC, DMF, RT, 16 h; (e) Ln(OAc)₃, DMF, RT, 4 h, quant.

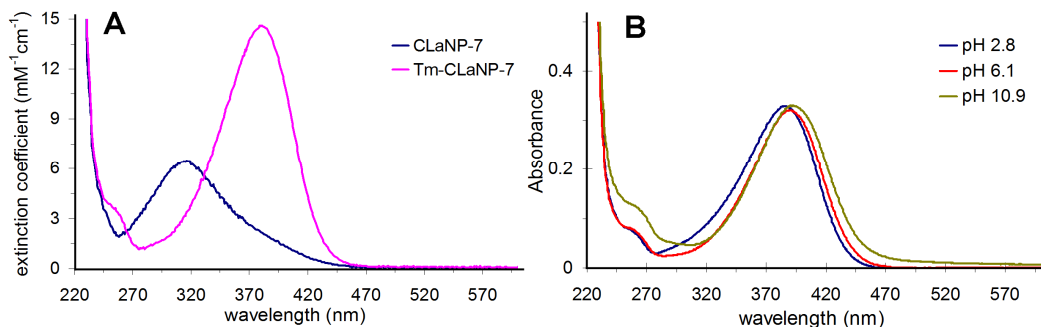


Figure 2. Electronic absorption spectra of CLaNP-7. (A) The absorbance spectra expressed as extinction coefficients are plotted for CLaNP-7 and Tm-CLaNP-7. (B) Lu-CLaNP-7 at different pH values.

Probe attachment and $\Delta\chi$ -tensors calculation:

The Zn²⁺-form of ¹⁵N-enriched E51C/E54C pseudoazurin (Paz) was reduced with dithiothreitol (DTT), washed, and directly incubated with Ln-CLaNP-7 for 16 h at 4 °C. The tagged protein was purified using a Superdex 75 column (GE Healthcare). The mass of the resulting ¹⁵N-Paz Yb-CLaNP-7 (14503 ± 2 Da) agreed with the expected mass of 14503 Da, assuming 98% ¹⁵N enrichment. In the [¹⁵N-¹H]-HSQC spectra, there were no significant differences between untagged and Lu-CLaNP-7 tagged spectra, except for a few residues close to the attachment site, enabling the resonance assignments to be made by comparison with previous spectra.³¹ Large shifts of resonances were observed when the protein was tagged with either Yb-CLaNP-7 or Tm-CLaNP-7 (Figure 3). The ¹⁵N rich Paz were kindly provided by Ms. Anneloes Blok and Dr. Monika Timmer (Leiden University, Inst. Chemistry).

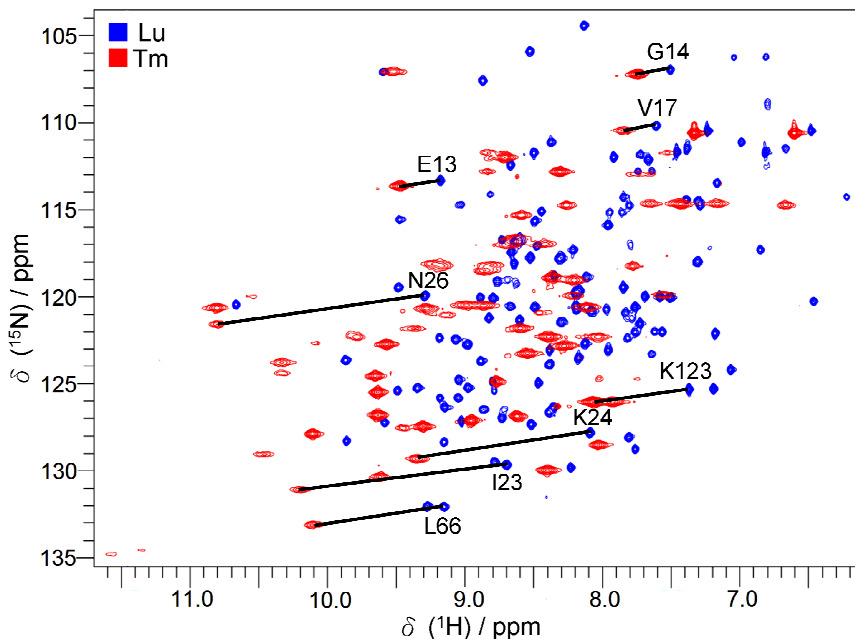


Figure 3. Overlay of $[^{15}\text{N}, ^1\text{H}]$ -HSQC spectra of Paz E51C/E54C attached to Lu-CLaNP-7 (blue) and Tm-CLaNP-7 (red). Several PCSs are indicated with solid lines.

The difference in resonance frequency between the paramagnetic and the diamagnetic samples was defined as the PCS. The presence of large, single PCSs indicates the tag to be attached rigidly and to exist in one dominant conformation, which is expected to be the SA isomer due to the six-member chelating system (but see Discussion section).³⁹

For estimation of the anisotropic component of the magnetic susceptibility tensor ($\Delta\chi$ -tensors), an initial metal position was fixed according to a previously reported protocol.¹¹ An initial set of PCSs was used to determine the $\Delta\chi$ -tensor, with which more PCSs were predicted. In an iterative way, the $\Delta\chi$ -tensor and metal position were refined and additional resonances were assigned. The $\Delta\chi$ -tensor values for Tm- and Yb-CLaNP-7, along with those of CLaNP-5 are reported in Table 1 and the back-calculated PCSs are plotted versus the observed PCSs in Figures 4A and Appendix 1, respectively. The values of $\Delta\chi_{ax}$ and $\Delta\chi_{rh}$ of CLaNP-7 are similar to those of CLaNP-5 for Tm^{3+} , but not for Yb^{3+} . The $\Delta\chi$ -tensor of Yb-CLaNP-7 is much more rhombic. A possible explanation could be the presence of a ninth ligand, a water molecule or hydroxyl ion. This possibility is discussed in more detail in the next section. Tm-CLaNP-7 causes significant alignment of Paz at 600 MHz (14.1 T),

allowing RDCs up to 20 Hz to be observed. The observed RDCs were used to optimize the HN positions of Paz and the $\Delta\chi$ -tensor derived from PCS was used to back-calculate the RDCs on the basis of this structure, yielding a good agreement (Figure 4B). The large RDCs indicate a low mobility of CLaNP-7 relative to the protein backbone.

Table 1. PCSs-based $\Delta\chi$ -tensors of CLaNP-5¹¹ and CLaNP-7^a

Protein	Probe	Ln	$\Delta\chi_{ax}^c$	$\Delta\chi_{rh}^c$	Restrains	Q ^b
Paz E51C/E54C	CLaNP-5	Tm	55.5 ± 0.8	10 ± 1	89	0.03
		Yb	9.4 ± 0.2	1.9 ± 0.4	93	0.04
	CLaNP-7	Tm	41.4 ± 0.6	9.6 ± 0.8	94	0.04
		Yb	4.2 ± 0.1	5.6 ± 0.4	93	0.06
Cyt <i>c</i> N56/L58C	CLaNP-7 (pH = 6)	Yb	6.3 ± 0.4	8.0 ± 0.3	70	0.03
		Yb	5.5 ± 0.9	9.6 ± 0.3	60	0.06
Cyt <i>c</i> N56C/L58C/H39A	CLaNP-7 (pH = 6.3)	Yb	5.5 ± 0.2	6.5 ± 0.1	70	0.04
		Yb	5.5 ± 0.1	6.1 ± 0.1	62	0.04

^a The unit of axial and rhombic components ($\Delta\chi_{ax}$ and $\Delta\chi_{rh}$) is 10^{-32} m^3 .

^b The definition of Q is given in experimental section (eq 2).

^c The error is calculated by a jackknife procedure randomly removing 20% of the data and repeating the $\Delta\chi$ -tensor fit 100 times.

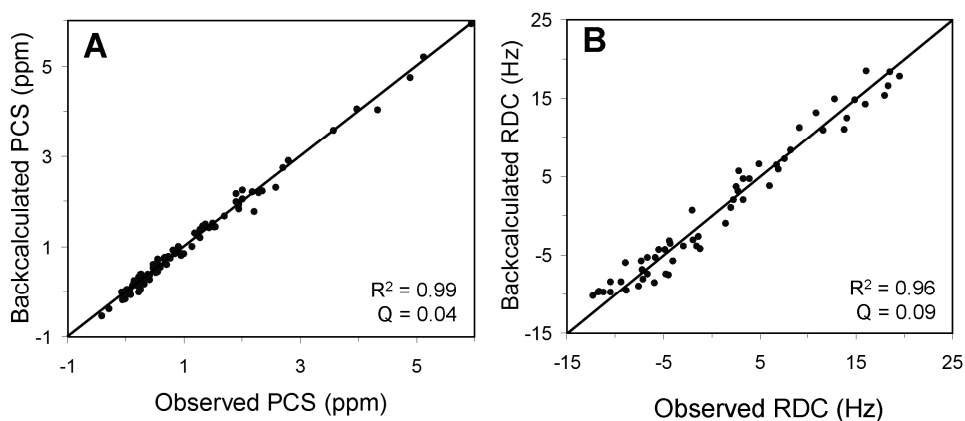


Figure 4. Experimentally observed amide proton PCSs and RDCs of Paz E51C/E54C Tm-CLaNP-7 plotted against the back-calculated PCSs (A, $Q = 0.04$) and RDCs (B, $Q = 0.09$), both based on the PCS derived $\Delta\chi$ -tensor. The NMR spectra were recorded at 14.1 T (600 MHz). The solid line represents a perfect match.

The pH dependence of CLaNP-7

In order to test CLaNP-7 on a second protein, yeast cytochrome *c* (Cyt *c*) N56C/L58C was tagged with CLaNP-7 coordinated to Yb³⁺ and Lu³⁺. In the diamagnetic spectrum (Lu-CLaNP-7) only single peaks were observed. However, at pH 7, the Cyt *c* tagged with Yb-CLaNP-7 showed two sets of peaks for most residues. The relative intensity and sometimes the sign as well changed with pH (Figures 5 and Appendix 2). From the PCSs obtained at pH 6 and pH 8, the $\Delta\chi$ -tensors were determined. A comparison of the PCSs shows that they differ significantly (Appendix 3). The sizes of the axial and rhombic components are similar at both pH values and somewhat larger than for Paz E51C/E54C (Table 1 and Appendix 4). The major difference between pH 6 and 8 is the orientation of the tensors (Figure 6A). The structurally highly similar tag Ln-CLaNP-5 shows a single set of resonances when attached to the same double Cys mutant of Cyt *c* (Appendix 5).⁹⁸ Also for CLaNP-7 attached to Paz E51C/E54C no pH dependence of the PCS was observed, so the observed effect is specific for CLaNP-7 attached to Cyt *c* N56C/L58C. The ¹⁵N rich Cyt *c* were kindly provided by Ms. Anneloes Blok and Dr. Monika Timmer (Leiden University, Inst. Chemistry).

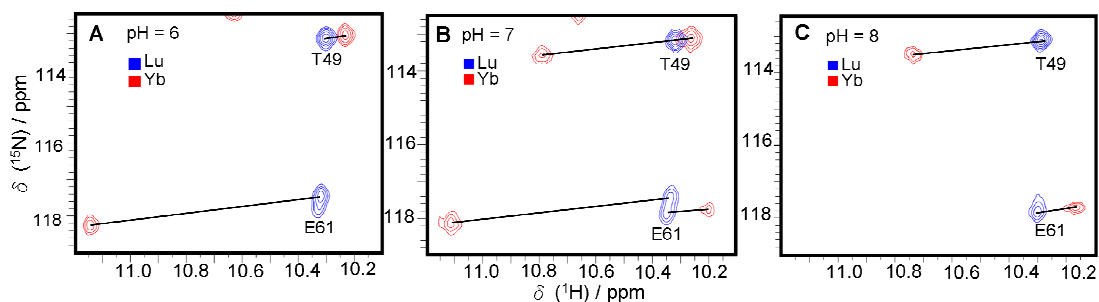


Figure 5. pH dependence of CLaNP-7. Detail of [¹⁵N, ¹H]-HSQC spectra of Cyt *c* N56C/L58C attached to Lu-CLaNP-7 (blue) and Yb-CLaNP-7 (red) at pH = 6.0 (A), pH = 7.0 (B) and pH = 8.0 (C).

Protonation of the phenol moiety of CLaNP-7 as an explanation for the pH dependence was ruled out by the electronic absorption spectrum. Protonation of the phenol shifts the absorbance maximum from 390 nm to 310 nm.¹⁴⁴ From Figure 2A, it is clear that in free CLaNP-7 purified by HPLC the phenol rings are protonated, but upon coordination to Tm³⁺ they are deprotonated at pH values between 3 and 11 (Figure 2B). In general, there is a water coordinated to the DOTA-like lanthanoid

ions complex in solution state.¹⁴⁵ The factors that affect water coordination are mainly the charge density of the lanthanoid ion and the steric strain at the water binding site.¹⁴⁶⁻¹⁴⁸ The substitution of the pyridine-*N*-oxide rings in CLaNP-5 with *p*-nitrophenol rings in CLaNP-7 lowers the charge of the coordinated oxygen of the ligand, which results in a larger space for a ninth coordination.^{39,43} Thus, it is likely that a water molecule or hydroxyl ion can be coordinated to the lanthanoid.

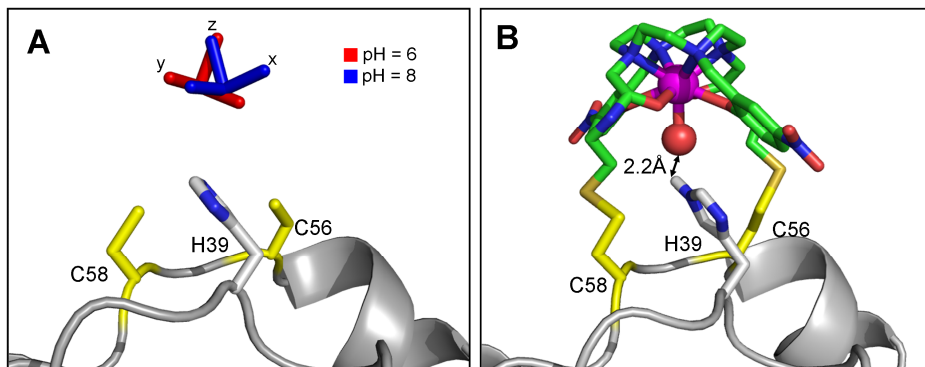


Figure 6. PCS-based positions of the tensor relative to the Cyt *c* structure with PDB entry code 1YCC.¹¹⁸ The Cys residues at positions 56 and 58 were modeled. (A) The principal axes of the $\Delta\chi$ -tensor of Yb-CLaNP-7 are shown as red (pH 6) and blue sticks (pH 8); (B) Model of CLaNP-7 attached to Cyt *c* N56C/L58C. The position of the Yb³⁺ (magenta) is derived from a fit to the PCS data. The red sphere shows the H₂O/OH at the ninth coordination position. The protein main chain is shown in grey. The Cys (N56C/L58C) and the His 39 side-chains are shown in CPK colors. The carbon atoms from CLaNP-7 are shown in green, nitrogen atoms in blue, oxygen atoms in red and sulfur atoms in yellow. The distance between the H^{ε2} of His 39 and the ligating oxygen atom is 2.2 Å.

In Cyt *c* N56C/L58C the Cys residues are located in a short β -strand and there is a histidine residue, His 39, in the neighboring strand, close to the tag attachment site. Fitting of the PCSs placed the lanthanoid close to His 39 and its imidazole ring can be rotated to be at hydrogen bond distance of a water molecule at the ninth coordination position (Figure 6B). Therefore, we propose that the observed pH dependence of the $\Delta\chi$ -tensor is caused by the imidazole of His 39.

In order to test this hypothesis, the His residue in Cyt *c* N56C/L58C was mutated to alanine and this variant was labeled with Ln-CLaNP-7. The pH dependence of the $\Delta\chi$ -tensor is no longer observed in the absence of the imidazole ring. The [¹⁵N, ¹H]-HSQC spectra shows single peaks at several pH values

(Appendix 6A) and the PCS and the $\Delta\chi$ -tensors are the same at low and high pH (Table 1 and Appendix 7). The peaks only exhibit small shifts due to the normal pH dependence of the protein and those shifts are identical in paramagnetic and diamagnetic samples (Appendix 6B). These observations support the proposal that His 39 influences the $\Delta\chi$ -tensor in a pH dependent manner. The ^{15}N rich Cyt *c* H39A/N56C/L58C were kindly provided by Ms. Anneloes Blok and Dr. Monika Timmer (Leiden University, Inst. Chemistry).

We wondered whether it was possible to introduce the pH dependence of the tensor by positioning the probe close to a His residue on a protein surface. For this purpose we returned to Paz, which is a β -sheet protein. His 6 is located on a long β -strand. In the neighboring strand two Cys residues were engineered, mutant I34C/V36C. The ^{15}N rich Paz I34C/V36C were kindly provided by Ms. Anneloes Blok and Dr. Monika Timmer (Leiden University, Inst. Chemistry). Using the published protocol for modeling of the CLaNP lanthanoid position,¹¹ it was predicted that the imidazole ring of His 6 would be sufficiently close to form a H-bond to a possible $\text{H}_2\text{O}/\text{OH}$ at the ninth coordination position (Appendix 8). The HSQC spectra clearly show two peaks for most resonances in this Paz variant labeled with Yb-CLaNP-7 and the intensity of these peaks indeed varies with pH, analogous to what was observed for Cyt *c* N56C/L58C (Figure 7). Note that Paz E51C/E54C labeled with CLaNP-7 did not show pH dependence. These results indicate that the pH dependence of the $\Delta\chi$ -tensor can be introduced when the probe is positioned on a β -sheet, next to a histidine residue. The pH dependence of CLaNP-7 may be used to obtain two independent sets of PCSs or RDCs from a single probe.

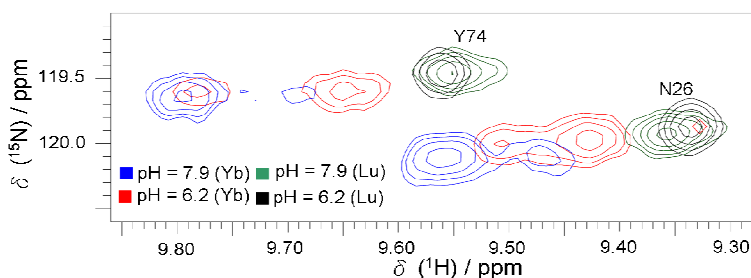


Figure 7. Detail of [^{15}N , ^1H]-HSQC spectra of Ln-CLaNP-7 tagged ^{15}N -labeled Paz I34C/V36C. The spectra were recorded at pH 6.22 (black, Lu; red, Yb) and pH 7.9 (green, Lu; blue, Yb).

Discussion

Proposed mechanism for CLaNP-7 pH dependence

Based on the $\Delta\chi$ -tensor, the position of the Yb-CLaNP-7 linked to Cyt *c* N56C/L58C is the same within error at pH 6 and 8. However, the orientations of the tensors are different (Figure 6A). The two sets of peaks in the HSQC spectra of Yb³⁺ labeled protein indicate that these orientations are a consequence of two orientations/conformations of the probe that are in slow exchange on the NMR chemical shift timescale. In contrast to what is expected for a simple pH titration in which the two sets of peaks would correspond to a protonated and deprotonated form, here both sets of peaks remain (weakly) visible, even at the highest and lowest pH values applied. Furthermore, not only do the relative intensities of the pairs of peaks change with pH, the PCSs of both states also exhibit some pH dependence (Appendix 9).

In order to explain these observations, a four-state model is invoked (Figure 8). The model hypothesizes that the two-fold symmetry of the probe is broken by the interaction between the imidazole of the nearby histidine and the proposed H₂O/OH coordinated to the Yb³⁺. Consequently, the two SA enantiomers ($\Delta\lambda\lambda\lambda\lambda$ and $\Lambda\delta\delta\delta\delta$) no longer yield identical PCS and now cause double peaks, because cyclen ring flips are normally slow.^{149,150} Protonation/deprotonation of the imidazole shifts the equilibrium between these two states. It also causes the pH dependence of the PCSs of both states (Appendix 9). The intensity ratio (I_b/I_a) of the pairs of peaks can be described on the basis of this model by eq. 1:

$$\frac{I_b}{I_a} = K \frac{[1 + 10^{(pH - pK_{a2})}]}{[1 + 10^{(pH - pK_{a1})}]} \quad \text{eq.1}$$

Where I_a and I_b are the peaks intensity of the two sets of peaks and I_b is most intense at high pH, K is the equilibrium constant, and pK_{a1} and pK_{a2} are the proton association constants. Fitting the observed intensity ratio of the peaks for Cyt *c* N56C/L58C to eq. 1 yields the curve given in Figure 8B. The equilibrium changes from $K = 0.52$ to $K' = 3.36$, where $K' = K(K_{a1}/K_{a2})$, so state III becomes the dominant conformation when going from high to low pH. For Paz I34C/V36C the effect is also clearly present, although the shift in the equilibrium is smaller (Figure 8B). The equilibrium rates were kindly calculated by Dr. Mathias A. H. Hass (Leiden University, Inst. Chemistry).

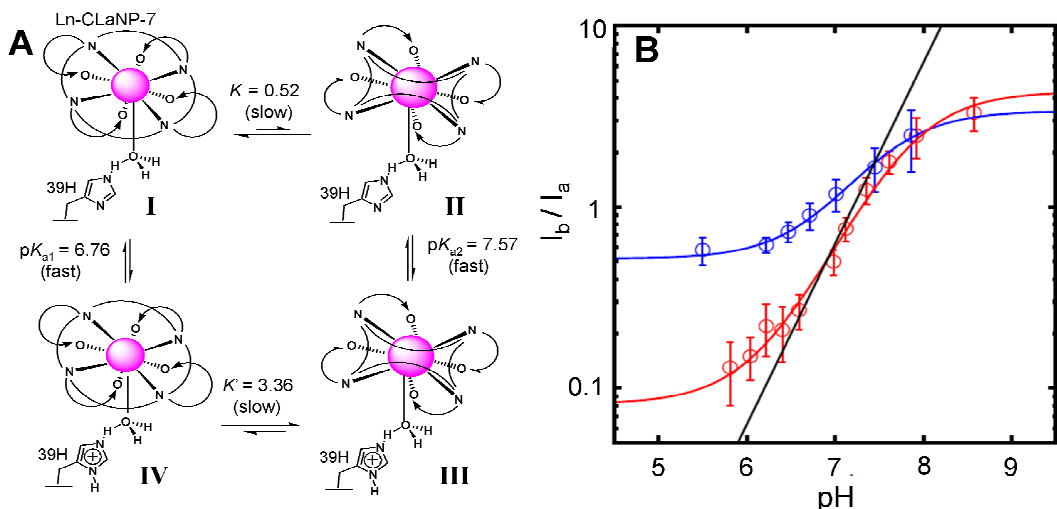


Figure 8. Proposed model to describe pH dependence of CLaNP-7. (A) The flip between two SA forms ($\Delta\lambda\lambda\lambda\lambda$ and $\Lambda\delta\delta\delta\delta$) are schematically represented by a change in the cyclen ring (lines connecting the N atoms) and the ligand arms (round arrows). The values were obtained from a fit to the I_b/I_a ratios of Cyt *c* N56C/L58C at multiple pH values (eq. 1). (B) Intensity ratios as a function of pH. The averaged intensity ratios for pairs of resonances in Cyt *c* N56C/L58C (red) and Paz I34C/V36C (blue) are plotted as a function of pH. The solid lines represent fits to the model described in the text (eq. 1). The intensity ratios are averaged from 13 residues for Cyt *c* and 10 residues for Paz and the error bars are the standard deviation. The black line represents a standard deprotonation curve.

Comparison with CLaNP-5

Tm-CLaNP-5 and Tm-CLaNP-7 were attached to Paz E51C/E54C and both cause large PCSs and RDCs, but these shifts and couplings differ in size and sometimes sign as well (Appendix 10). The position of the metal, as well as the size and orientation of the $\Delta\chi$ -tensor were obtained by fitting to the PCS data. The PCS histograms have an overall similar appearance for both tags because PCS is dominated by the distance between the nucleus and the metal. However, detailed inspection shows clear differences that reflect the somewhat smaller size and changed orientation of the CLaNP-7 $\Delta\chi$ -tensor. Also the positions of the Ln-ions are different by 3.4 Å (Figure 9C). The RDC histograms show many more differences (Appendix 10B), because RDC is solely dependent on the H-N bond vector orientation in the $\Delta\chi$ -tensor frame. The RDCs range from -15 Hz to +20 Hz for Tm-CLaNP-7 and from -20 Hz to +30 Hz for Tm-CLaNP-5 at 14.1 T (600 MHz). The

observed PCSs and RDCs of CLaNP-7 were plotted versus the observed PCSs and RDCs of CLaNP-5 (Figure 9) and show poor agreements between CLaNP-5 and CLaNP-7. It is concluded that the two probes cause sufficiently different effects to yield complementary structural restraints from a single attachment site.

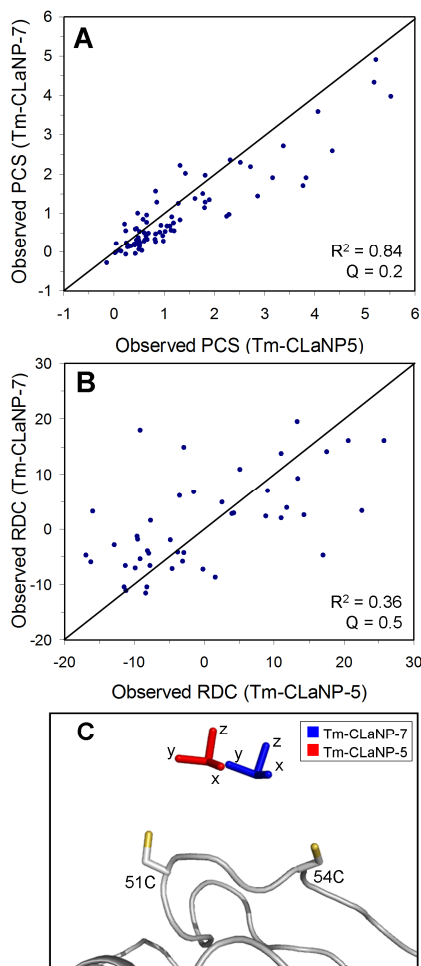


Figure 9. Comparison of CLaNP-5 and CLaNP-7. Experimentally observed PCSs and RDCs from Tm-CLaNP-7 plotted against the experimentally observed PCSs (A, $Q = 0.2$) and RDCs (B, $Q = 0.5$) from Tm-CLaNP-5 for Paz E51C/E54C. The solid line represents a perfect correlation. (C) Experimentally determined position and orientation of the Tm³⁺ $\Delta\chi$ -tensor relative to the Paz (PDB: 1PY0)³¹ structure for CLaNP-5 (red sticks) and for CLaNP-7 (blue sticks). The Cys side-chains are shown in CPK colors.

Conclusion

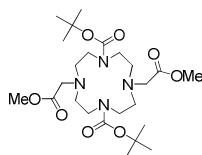
CLaNP-7 is a new two-armed lanthanoid chelating protein probe that provides large PCSs and RDCs. CLaNP-7 and CLaNP-5 have different magnetic susceptibility tensors, providing a convenient way to obtain different paramagnetic effects from the same target protein with a single set of engineered Cys residues. In addition, the lower net charge of CLaNP-7 will be beneficial in protein-protein interaction studies. CLaNP-7 has a bright yellow color simplifying the sample handling, and importantly, it is the first example of a pH sensitive paramagnetic probe offering a unique opportunity to tune paramagnetic effects.

Experimental Section

General

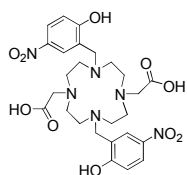
$\text{Ln}(\text{OAc})_3$, cyclen, 2-(aminoethyl)methanethiosulfonate hydrobromide, 2-hydroxy-5-nitrobenzyl bromide and all other chemicals were used as purchased without further purification. TLC-analysis was conducted on DC-alufolien (Merck, Kieselgel60, F254) with detection by UV-absorption (254 nm). Flash chromatography was performed on Screening Devices silica gel 60 (0.04-0.063 mm). A Biocad Vision HPLC (PerSeptive Biosystems, inc.) and an Akta Basic FPLC (GE Healthcare Inc.) were used for purifications. Analytical, semipreparative, and preparative reversed phase C18 columns were obtained from Phenomenex (Torrance, CA). Superdex 75, CM sepharose and HiTrap SP columns were obtained from GE Healthcare. NMR spectra were recorded on a Bruker AV-400 (400/100 MHz) and Bruker Avance-III 600 (600/150 MHz) spectrometer. A LCQ LCMS system and a Finnigan LTQ Orbitrap system were used for HRMS and protein conjugation analysis. FTIR was performed on a Perkin-Elmer (Shelton, CT) Paragon 1000 FTIR spectrometer. Melting points were obtained using a SMP3 scientific melting apparatus (Stuart, Bibby Sterlin Ltd.)

1,7-diBoc-1,4,7,10-tetraazacyclododecane-4,10-dimethyl acetate (1)



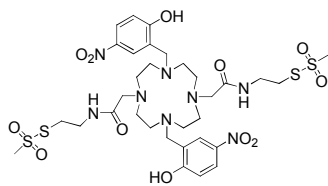
BocOSu (2.49 g, 11.6 mmol) was dissolved in dry CHCl_3 (20 mL) and was added under argon to a cyclen (1 g, 5.8 mmol) solution in CHCl_3 (40 mL). The reaction mixture was stirred at room temperature for 36 h. To the reaction mixture 3 M NaOH (30 mL) was added and

stirring was continued for 30 min. Brine (30 mL) was added and the solution was extracted with dichloromethane (3 x 20 mL). The organic fractions were combined, dried over MgSO₄ and concentrated *in vacuo*. The remaining colorless oil was dissolved in acetonitrile (30 mL). K₂CO₃ (1.94 g, 14.5 mmol) and methyl 2-bromoacetate (2.22 g, 14.5 mmol) were added into the solution and stirred for 12 h at room temperature. The reaction mixture was concentrated, dissolved in ethyl acetate and washed with brine. The organic layer was dried (MgSO₄), filtered and concentrated. The resulting residue was purified by column chromatography to yield compound **1** as a white amorphous solid (2.48 g, 83% yield). m. p. = 82–83 °C. R_f = 0.3 (5% MeOH in DCM). ¹H NMR (400 MHz CDCl₃): δ = 1.27 (s, 18H), 2.69 (br, 8H), 3.21 (br, 8H), 3.28 (s, 4H), 3.51 (s, 6H). ¹³C NMR (100 MHz CDCl₃): δ = 28.14, 46.21, 50.98, 54.36, 54.54, 79.05, 155.51, 171.39. FTIR: 2975.8, 1739.6, 1683.9, 1364.7, 1157.3 cm⁻¹. HR-MS m/z: 517.3225 [M+H]⁺, calcd [C₂₄H₄₅N₄O₈]: 517.3232.



1,7-dimethylene-(*p*-nitrophenol)-1,4,7,10-tetraazacyclo-dodecane-4,10-diacetic acid (3**)**

Compound **1** (400 mg, 0.75 mmol) was dissolved in a mixture of dichloromethane and trifluoroacetic acid (4 mL, 1:3 v/v) and stirred for 4 h at room temperature. The reaction mixture was concentrated under reduced pressure and coevaporated with toluene to remove the trifluoroacetic acid. The crude mixture was dissolved in acetonitrile (10 mL). 2-hydroxy-5-nitrobenzyl bromide (435 mg, 1.88 mmol) and K₂CO₃ (260 mg, 1.88 mmol) were added into the solution, which was stirred for 12 h at 80 °C. The reaction mixture was filtered and the solid was washed with acetonitrile (30 mL). The filtrate was concentrated *in vacuo* to give a yellow oil. The crude compound was dissolved in a solution mixture which contained 1,4-dioxane (final concentration was 15 mM) and 3 M NaOH (final concentration was 0.4 M). The solution was stirred at room temperature for 4 h, then concentrated under reduced pressure and purified by HPLC (0.1% TFA and a 10–50% acetonitrile gradient on C18 preparative column). ¹H NMR (400 MHz CD₃OD): δ = 3.19 (s, 8H), 3.33 (s, 4H), 3.44 (s, 8H), 4.64 (s, 4H), 7.12 (d, 2H), 8.30 (d, 2H), 8.54 (s, 2H). ¹³C NMR (100 MHz CD₃OD): δ = 174.71, 164.29, 142.31, 130.87, 129.33, 117.59, 117.39, 54.15, 51.57, 49.87. FTIR: 3084.3, 1728.1, 1667.9, 1593.1, 1496.0, 1338.9, 1286.1, 1185.8, 1133.0, 1084.8 cm⁻¹. HR-MS m/z: 591.2409 [M+H]⁺, calcd [C₂₆H₃₅N₆O₁₀]: 591.2409.



CLaNP-7

Compound **3** (296 mg, 0.5 mmol) was dissolved in *N,N*-dimethylformamide (10 mL) and treated with 2-(aminoethyl)methanethiosulfonate hydrobromide (283.4 mg, 1.2 mmol), *N*-hydroxysuccinide (345.3 mg, 3 mmol) and *N*-(3-dimethylaminopropyl)-*N'*-ethylcarbodiimide (574.5 mg, 3 mmol). The reaction mixture was stirred 16 h at room temperature. The reaction mixture was concentrated under reduced pressure and purified by HPLC (0.1% TFA and a 20-45% acetonitrile gradient on C18 preparative column) yielding **CLaNP-7** (40%) as a yellow oil. ¹H NMR (600 MHz, d⁶-DMSO, 323 K): δ = 3.09 (s, 8H), 3.21 (s, 4H), 3.27 (s, 8H), 3.31 (t, 4H), 3.47-3.53 (br, m, 10H), 7.12 (d, 2H), 8.21 (q, 2H), 8.47 (s, 2H), 8.51 (s, 2H). ¹³C NMR (150 MHz, d⁶-DMSO, 323 K): δ = 34.87, 38.21, 48.68, 49.80, 50.17, 51.52, 53.92, 116.40, 127.11, 129.22, 139.12, 164.06, 169.98. FTIR: 3465.8, 1649.8, 1138.9, 1198.9, 1134.5, 1100.8 cm⁻¹. HR-MS m/z: 865.2358 [M+H]⁺, calcd [C₃₂H₄₉N₈O₁₂S₄]: 865.2347.

Lu-CLaNP-7

Lu(OAc)₃ (2.37 mg, 5.38 μmol) and CLaNP-7 (4.19 mg, 4.84 μmol) were separately dissolved in *N,N*-dimethylformamide (50 μL). Then, the CLaNP-7 solution was added into Lu(OAc)₃ solution and stirred for 4 h at room temperature. Without further purification, Lu-CLaNP-7 was used to label protein samples. The other lanthanoid ions Yb³⁺, and Tm³⁺ were chelated to CLaNP-7 following the same procedure. HR-MS m/z: 1036.1513 [M]⁺, calcd [C₃₂H₄₆N₈O₁₂S₄Lu]: 1037.1520.

Protein production and purification

The production and purification of the ¹⁵N enriched *Alcaligenes faecalis* pseudoazurin (Paz) double cysteine mutant E51C/E54C was performed as described before,³¹ with small modifications. Instead of *Escherichia coli* BL21 (DE3), *E. coli* BL21 (PlysS) was used to produce Paz E51C/E54C and Tris-HCl buffer (20 mM Tris-HCl, pH 7.0) was used for ion exchange chromatography on the CM column. Double cysteine mutations I34C/V36C were prepared by the QuikChange method using the expression plasmid of wt Paz as a template.¹⁵¹ The oligonucleotides 5'-GGCGACACGGTCACCTTTTGTCCG TGCGACAAAGGACATAATG-3' and its

complement were used as the forward and reverse primers, respectively. The expression and purification of the ^{15}N enriched variant was performed using the same conditions as described above. The final yield obtained for Paz I34C/V36C was 2.4 mg/L of culture. ^{15}N enriched yeast Cyt *c* N56C/L58C was produced and purified by the published method.⁹⁸ To create mutant Cyt *c* H39A/N56C/L58C, the forward and backward primers 5'-CTTGCATGGTATCTTTGGCAGAGCCTCTG GTCAAGCTGAAGGGTATTTCG-3' and its complement were used on the template encoding Cyt *c* N56C/L58C. Expression and purification was identical to that of N56C/L58C. The final yield was 2.8 mg/L of culture.

Paramagnetic Probe Attachment

To attach Ln-CLaNP7 to Paz and Cyt *c*, protein sample (1 mL, 150-300 μM) was treated with DTT (final concentration 5 mM) at 0 °C for 1 h to remove possible dimers. The reaction mixture was loaded on a PD-10 column (GE Healthcare) pre-equilibrated with labeling buffer (20 mM sodium phosphate, 150 mM NaCl and pH 7.0) to remove DTT. To avoid any reoxidation by air, the buffer was degassed and the PD-10 column kept under an argon atmosphere. To the eluted protein five equivalents Ln-CLaNP-7 were added. The solution was stirred 16 h at 4 °C. The probe attached Paz sample was concentrated to 500 μL and purified over a Superdex 75 gel filtration column. In the case of Cyt *c*, the protein was purified on a HiTrap-SP column. The yield of labeling, estimated from the intensity of diamagnetic peaks in the [^{15}N , ^1H]-HSQC spectra of samples with paramagnetic tags, was more than 90%.

NMR spectroscopy

The NMR samples of Paz Ln-CLaNP-7 (100-200 μM) were prepared in 20 mM sodium phosphate, 150 mM NaCl buffer and 6% (v/v) D_2O . All Cyt *c* samples (100-200 μM) contained 20 mM sodium phosphate buffer, 6% (v/v) D_2O and one eq. of ascorbic acid under an argon atmosphere to keep the Cyt *c* in the reduced state. The pH of these samples was set with small aliquots of 0.1 M HCl or 0.1 M NaOH and was checked before each titration point. All [^{15}N , ^1H]-HSQC and IPAP spectra¹⁵² were recorded at 298 K on a Bruker Avance III 600 MHz spectrometer. Data were processed with NMRPipe¹⁵³ and analyzed with CCPNMR Analysis version 2.1.¹⁵⁴ Assignments of the resonances were based on previous work.^{99,155 31}

PCS and RDC analysis

PCS were defined as the chemical shift difference for a resonance in the paramagnetic and diamagnetic sample. Positioning of the metal and optimization of the $\Delta\chi$ -tensor were performed as described for CLaNP-5,¹¹ by using XPLOR-NIH version 2.9.9¹⁵⁶ and Pararestraints.¹⁵⁷ The manuscript for XPLOR-NIH and the calculation of $\Delta\chi$ -tensor were kindly performed by Dr. Peter H. J. Keizers (Leiden University, Inst. Chemistry). The structures of Paz and Cyt *c* were taken from PDB entries 1PY0 and 1YCC and hydrogens were added.^{31,118} The variation in the Ln positions were calculated by randomly removing 20% PCS data and repeating the $\Delta\chi$ -tensor fit 100 times. For RDC analysis, the HN positions were optimized on the basis of the experimental RDCs. The optimized structure was used for back-calculation of the RDCs on the basis of the PCS-derived $\Delta\chi$ -tensor. The Q factor provides a normalized measure for the agreement between a set of observed and calculated experiment data. The Q factor was defined as eq. 2.¹⁵⁸

$$Q = \sqrt{\sum_i (O_i^{obs} - O_i^{calc})^2 / \sum_i (O_i^{obs} + O_i^{calc})^2} \quad \text{eq. 2}$$

where O_i^{obs} and O_i^{calc} are the observed and calculated PCSs or RDCs.